Day-ahead profit-based reconfigurable microgrid scheduling considering uncertain renewable generation and load demand in the presence of energy storage

Hemmati , Mohammad ; Mohammadi-ivatloo, Behnam; Abapour, Mehdi; Anvari-Moghaddam, Amjad

Published in:
Journal of Energy Storage

DOI (link to publication from Publisher):
10.1016/j.est.2019.101161

Publication date:
2020

Document Version
Accepted author manuscript, peer reviewed version

Day-Ahead Profit-based Reconfigurable Microgrid Scheduling Considering Uncertain Renewable Generation and Load Demand in the Presence of Energy Storage

Mohammad Hemmati [1], Behnam Mohammadi-ivatloo[1], Mehdi Abapour [1], Amjad Anvari-Moghaddam[2]

[1] Faculty of Electrical and Computer Engineering, University of Tabriz, Tabriz, Iran

[2] Department of Energy Technology, Aalborg University, Aalborg, Denmark

Abstract: Due to the penetration of renewable energy sources (RESs) with probabilistic natures into microgrids (MGs), optimal scheduling and reconfiguration (RG) processes are associated with uncertainty. This paper presents the stochastic profit-based optimal day-ahead scheduling of a reconfigurable microgrid (RMG) as a new generation of the conventional microgrid. The proposed algorithm finds the optimal RMG's topology from the profit maximization point of view, the optimal hourly MG's unit set-points like micro-turbines (MTs) and energy storage, and power exchange with the main grid, simultaneously. The generated power of wind turbine (WT) and PV panel, as well as load demand are considered as uncertain parameters. To solve the profit maximization problem of RMG, *time-varying acceleration coefficients* particle swarm optimization (TVAC-PSO) algorithm is employed. Also, to ensure simulation accuracy in the presence of high-level uncertainties, the autocorrelation model is used based on actual data for the uncertainty of renewable power output. The feasibility and applicability of the proposed framework are demonstrated on a 69-bus radial RMG with various distributed generators in different cases. The results show the effectiveness of the proposed model.

Keywords: Reconfigurable microgrid, energy storage, hybrid energy system, optimization

1. Introduction

The Microgrid (MG) is a small/medium-scale distribution network consists of multiple loads (controllable and non-controllable), generation units (dispatchable and non-dispatchable), energy storage systems (ESSs), and switches that are working under dedicated controllers supervision [1, 2]. MG can provide significant advantages such as reliability improvement, ancillary services, operation cost reduction, mitigation environment emission loss reduction and power quality improvement [3, 4]. To achieve these goals, multiple control methods are needed. However, one of the most effective methods for MG structure controlling is reconfiguration (RG). RG is the process of topology alteration by using normally opened or closed switches.

In the conventional distribution networks, RG is implemented for a few purposes such as minimizing power loss and voltage regulation, reliability and restoration improvement, load balancing [5, 6]. In comparison with the conventional networks, RG is not only used for a simple restructuring by changing the switches status in MGs. For example, the RG can be used to cluster a MG into a set of smaller energy systems (or multi-microgrids) in case of emergency conditions. Furthermore, it is expected that future distribution networks will consist of several interconnected MGs [7], where control of neighbouring MGs through RG process can be a suitable and feasible solution for system operation management.

The development of smart grid concept alongside information technologies can result in simplification of the controlled process of MGs. Remote controlled and programmable switches are among those technologies which facilitate the RG process. Add the ability to change the structure according to the MG condition, created the new generation of MG, named RMG. Unlike conventional MG, RMG has a higher degree of freedom. Recently, RMG attracted much interest. In [8], risk-based scheduling of RMGs in the presence of wind turbines is presented. The wind power generation and

power exchange price with the upstream network are considered as uncertain parameters while TVAC-PSO algorithm is implemented to find the optimal structure at each time. Authors in [9], expressed that future distribution system contains neighbouring MGs which can exchange the power together. For this purpose, the connection between MGs is provided in two levels and the RG process is implemented for the MG coupling. The proposed algorithm finds the optimal connectivity between the MGs based on surplus and unserved energy level in each one while passing through both reliability and power loss indices. In [10], day-ahead scheduling and hourly reconfiguration of smart distribution system considering the load demand and wind power uncertainties is studied. The scenario-based approach is used to model the uncertain parameters and the optimal hourly structure is find by using PSO algorithm while no limitation for the number of daily structure is considered. In [11], operation scheduling of MG with dynamic and adaptive hourly reconfiguration is presented. In this paper, for joint operational scheduling and hourly reconfiguration of MGs, a stochastic Model Predictive Control approach is developed. In [12] a new multi-objective formulation for MG operation in islanded mode is presented. The model behaves based on the probabilistic nature of renewable energy sources (RESs) and loads and considers minimum fuel cost and switching cost together with maximum loadability of feeders as objectives. The islanded MG reconfiguration is presented as a flexible tool to improve loadability and power loss minimization using an adaptive multi-objective harmony search algorithm. In [13], a vulnerability assessment is developed by using RG in both connected and islanded modes for MGs. The MG reconfiguration model is implemented with consideration of the both grid-connected and islanded modes and vulnerability assessment, by using a searching vector (SVAPO) algorithm. In [14], a day-ahead MG scheduling problem in the presence of RES and storage systems have been investigated. The proposed problem considering the AC power flow is formulated as a mixed-integer linear programming (MILP) and an adaptive robust

optimization method is implemented to address the uncertainties. The scenario-based stochastic approach for optimal CHP/ RES and hydrogen-based MG is presented in [15]. The uncertainties of RES, market price and strategy of storing the hydrogen convert the problem to a stochastic MINLP one. In [16], a day-ahead operation scheduling of RMG to minimize the power loss is presented. The selective PSO (SPSO) algorithm is proposed to find the optimal solution for controllable distributed generation and RCSs states, simultaneously.

By increasing the penetration of renewable energy as well as the variation of the load and power price, the MG optimal scheduling is associated with uncertain parameters [17]. Authors in [18] investigate a daily optimal scheduling problem of MGs by considering intermittent behaviour in generation and load. Likewise, a novel robust optimization approach is presented in [19] for optimal design of MGs in the presence of uncertainties considering reconfigurable topology. In [20], optimal scheduling for MG operation considering islanding capability constraint with uncertainty of PV, WT and load is proposed and solved by mixed-integer linear programming (MILP) techniques. In [21], a new probabilistic model for the MG operation is presented in the presence of uncertainty of WT power output. In [22], the optimal stochastic energy management of a retailer based on selling price under uncertainties of energy prices, demand, wind speed and irradiation is presented and scenario-based stochastic framework is used for uncertainty modelling. In [23], MG optimal scheduling is developed with multiple uncertain parameters such as a generated power of PV and wind, load demand and daily market price deviation. In the same study, $2m+1$ point estimation method is implemented for modelling uncertainties [24]. In [25], to investigate the effect of uncertainty on MG optimal operation, a new stochastic framework is presented. In this study, load forecasting errors, generated power of PV, WT and market price are considered as uncertain parameters. In [26], a stochastic approach to design a wind integrated energy hub with multiple energy systems is presented.

The wind power generation and load forecasting errors are considered as random variables and scenario-based approach is applied for uncertainty handling.

The literature review shows that optimal day ahead scheduling of MGs has been the subject of several studies and different mathematical and heuristic techniques have been developed to address this problem. However, the optimal scheduling of RMG have been studied by a limited number of researchers. Given that RMGs are deemed as the next generation of MGs with a higher degree of flexibility and scalability, more research is needed to be done in this area. Moreover, MG reconfiguration and optimal dispatch of units known as unit commitment (UC) should be considered simultaneously. Also, most of the reviewed literature on MG scheduling, have focused on modelling the uncertainties of load and generation using scenario-based approaches. However, there is still room to improve such techniques to better represent uncertainties and to report more accurate and realistic results in shorter time. In this paper, a day-ahead RMG profit-based optimal scheduling integrated with renewable energy sources and energy storage is presented. The main contribution of this paper is to use RG and UC to find the optimal set-points of units and RMG's topology, simultaneously. To address the high level of renewable power output uncertainties, the autocorrelation model is implemented. Using the autocorrelation model and metaheuristic approach based on *time-varying acceleration coefficients particle swarm optimization (*TVAC-PSO) algorithm can find the optimal state of variables in profit-based RMG scheduling problem in a reasonable time. It is expected that using the RG and UC for managing the RMG operation will bring a numerous economic benefits for its operator.

The rest of this paper is organized as follows: Section 2 provides the proposed models to address the uncertain parameters. Section 3 presents the formulation of the objective function in terms of costs and revenues and profit maximization for RMG. The proposed algorithm and contribution of

the TVAC-PSO algorithm is presented in Section 4. Section 5 contains numerical results and investigates the performance of the proposed model. Finally, the conclusion of the paper is presented in Section 6.

2. Uncertainty modelling

As mentioned, the penetration of RESs into MG could affect the system operation and planning states. Due to the probabilistic nature of wind speed and sun irradiance, the generated power of these resources are significantly fluctuating. Furthermore, the daily load behaviour emerges as an uncertain parameter. Therefore, the proposed optimal profit-based MG scheduling consists of a high number of uncertain parameters. The probabilistic analysis in the presence of multiple uncertainties is a powerful tool for the scheduling RMS. Therefore, to model the renewable power output and load demand uncertainties, the autocorrelation model and scenario-based stochastic approach are used, respectively, which are presented in this section.

2.1. Wind power output

The generated power by WT depends on wind speed. The probability distribution of wind power output varies with real output [27]. Based on the forecast and real power output of five turbines in KHAF wind farm with 66 wind turbines in 2015-2016 [28], a model of power output probability distribution will set up by fitting to Weibull distribution. For this purpose, three main steps are necessary:

1. The forecast data at each time normalized and rearranged in ascending order.
2. The series data in step 1 are divided into 100 groups. There is 0.01 p.u. power difference between adjoining groups.

3. For each group, the corresponding data of real generated power is fitted to the PDF of the Weibull distribution.

Using above steps, the PDF of wind power output can be obtained based on the day-ahead forecast output as following:

$$f\ (\mathrm{V}) = \frac{r}{c}\left(\frac{V}{c}\right)^{r-1} \exp\left[-\left(\frac{V}{c}\right)^{r}\right] \quad (1)$$

Where r and c are Weibull parameters, which calculated by the maximum likelihood estimation method for each group in step two [29]. Also, f is Weibull PDF and V is wind speed in *m/s*.

Autocorrelation model of wind power output: According to the real output power of KHAF station, it can be seen that there is temporary correlation in real data. To ensure the accuracy of simulation, we must consider the correlation in the wind power output. The steps of the proposed model are as follows:

1. At first, r and c (Weibull parameters) for 24 hours of day-ahead forecasted power output are estimated based on the previous section.
2. Two matrixes named X and $Y_T^{(0)}$ are generated by Latin hypercube sampling (LHS) simulation following the normal distribution. X and $Y_T^{(0)}$ are two 1000×24 matrixes that each column is composed of 1000 numbers to ensure its independence.
3. Let's consider R as an autocorrelation matrix. Using the Cholesky decomposition method and Nataf technique [29, 30], we can find C, where $R = CC^T$.
4. If $Y^{(0)} = \phi$, then $Y^{(d)} = \left[Y_T^{(d)}, X\right]C^T$, where d is d^{th} day of simulated data. Therefore, $Y^{(d)} = \left[Y^{(d-1)}, Y_1^{(d)}, ..., Y_T^{(d)}\right]$.
5. If D is the length of time series (in this paper, time series is one day), then the number of Y must be equal to $D.T$ (365×24), otherwise, $d = d + 1$ and the process goes to step 4.

6. By definition of $c_t = c_{t-T}$ and $r_t = r_{t-T}$, where $t = 1,2,.....DT$, normal Cumulative distribution function (CDF) of Y_t can be calculated as $F_n(Y_t)$.

7. In the last step, we define B_t matrix. *B* is the inverse CDF of the Weibull distribution at time interval *t* as $F_t^{-1}(F_n(Y_t))$. Actually, *B* contains 1000 forecast samples of time series of daily power generation of wind turbine.

With regard to the above steps to generate B, it can be concluded that the probability distribution of its columns and the characteristics of each row are almost identical. One of the rows of B is chosen randomly and considered as a wind power output.

2.2. PV power output

The generated power of PV depends on air temperature and solar radiation. These two parameters are different at any time. Fig. 1, shows the variety of irradiation in KHAF station for 118 days between 2008-2009 [28].

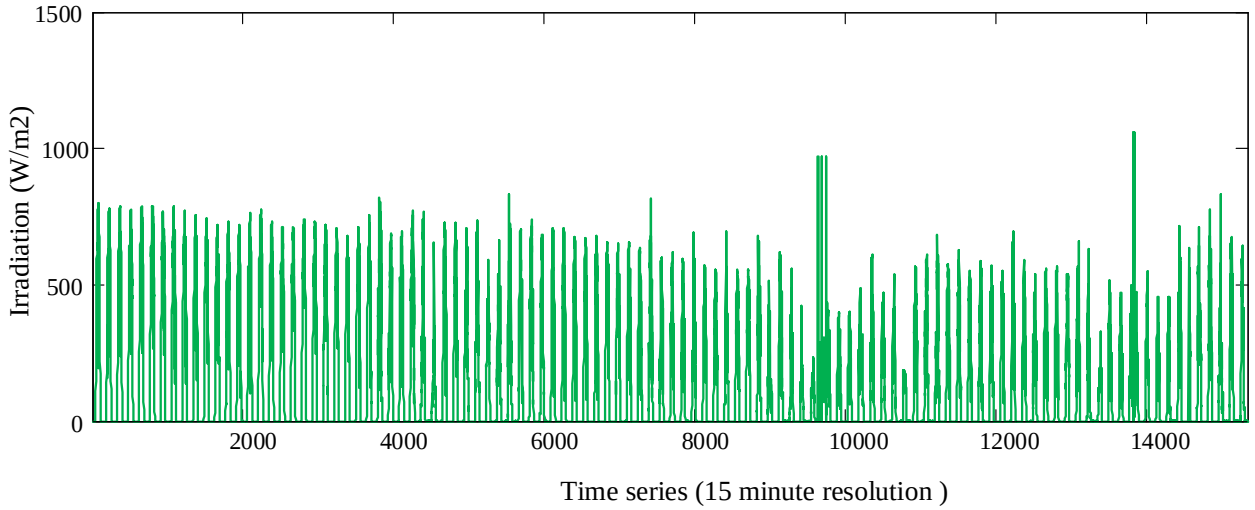

Fig. 1. The variety of irradiation in KHAF station.

Based on forecasted data, assumed that there is PV farm in KHAF. Therefore, a model of power output probability distribution will set up by fitting to the normal distribution. The form of normal distribution is:

$$f\ (P_{pv}) = \frac{1}{\sqrt{2\pi} \times \sigma} \exp\left(- \frac{((P_{pv}) - \mu)^2}{2 \times \sigma^2} \right) \quad (2)$$

Where $f\ (P_{pv})$ is normal PDF of the PV power output, P_{pv} is power output of PV panel in kW, σ and μ are standard deviation and the mean of the normal distribution, respectively.

All the steps mentioned about the autocorrelation model of wind power output are established for the PV power output. It should be noted that (parameters of normal distribution) are determined by maximum likelihood estimation method.

After calculation of normal PDF, the irradiation and air temperature are converted into power based on:

$$P_{pv} = P_{STC} \times \frac{G_{ING}}{G_{STC}} \times \left(1 + K\ (T_c - T_r)\right) \quad (3)$$

where P_{pv} and P_{STC} are output power of the module at irradiance G_{ING} and rated power at G_{STC} (standard condition in W/m^2), respectively. T_c and T_r are cell and air temperature in ^0C, respectively. *K* is maximum power temperature coefficient. The rated power of PVs (P_{STC}) is 250 kW.

2.3. Load demand

To model the uncertainty of load variation, we assume that is subjected to the normal distribution [18] like (2). Monte-Carlo simulation (MCS) generates a high number of scenarios subject to the Normal distribution that each of the scenarios are assigned a probability that is equal to one partitioned by the number of generated scenarios [31]. In each scenario, a random load demand is considered for each hour. Because the MCS generates a large number of scenarios, the variance of

scenarios is too much. The LHS is an adequate technique which can reduce the number of runs for MCS to achieve a precise random distribution. Furthermore, LHS can reduce the variance of MCS scenarios [31]. To demonstrate the effect of LHS for the variance of the MCS sampling reduction, an example is presented for a load demand subject to normal distribution with $\mu = 800\,kW$ and $\sigma = 10\,kW$. Fig 2 and 3 display the ordinary MCS and the MCS with LHS respectively. In both simulations, 1000 samples are considered. According to Fig 2 and 3, LHS can approximate the accurate distribution PDF much better than the ordinary MCS.

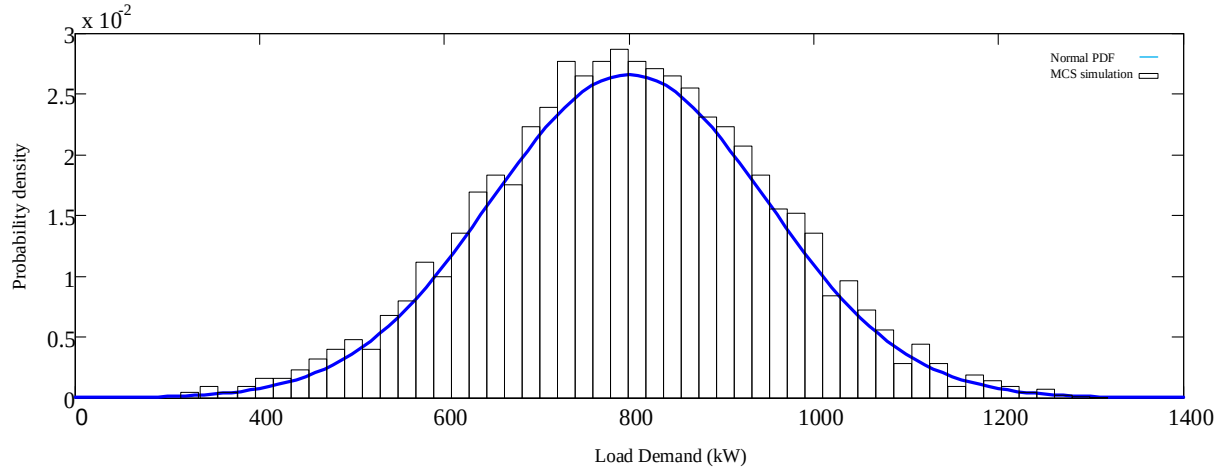

Fig. 2. Normal PDF fit by MCS.

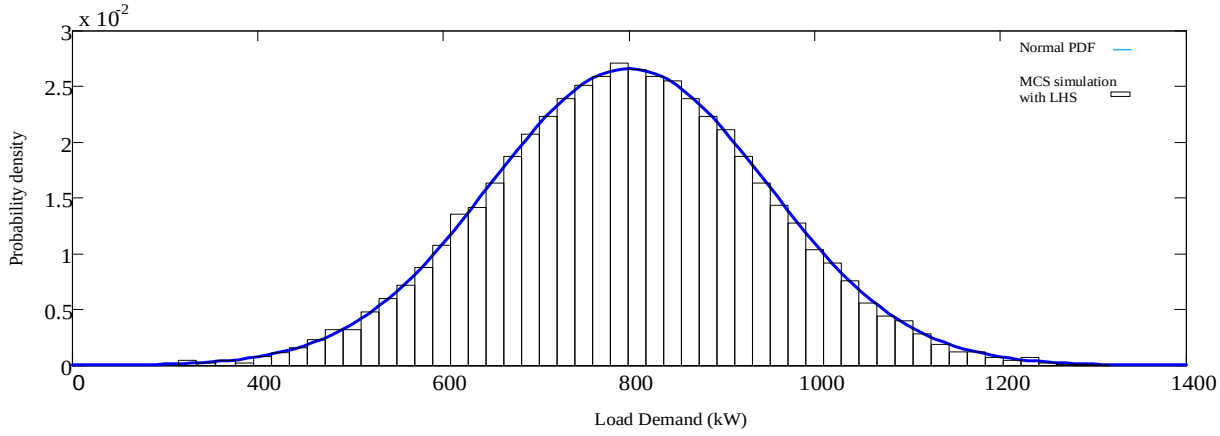

Fig. 3. Normal PDF fit by MCS with LHS.

3. Problem formulation

As previously mentioned, MG management using optimal UC and RG process can provide multiple advantages. RG could reroute the power from heavy-loaded parts to light-loaded parts by changing the MG's network topology. This action can also affect the power loss, power flows, commitment states of units, exchanged power and as a result the MG's costs and revenues. As previously mentioned, maximum economic profit for MG's owner is considered as an objective which is defined based on the difference between the revenue and the total cost. In order to take uncertainties into account, we generate different scenarios. After generating different scenarios for exiting uncertainty, the expected value of the profit for the day is calculated, in line with [32]. The objective function is expressed as follows:

$$Maximize \quad \text{Profit} = RV - TC \tag{5}$$

where RV is MG's owner revenue ($) and TC is total cost ($) of MG. The revenue for MG's owner is calculated according to:

$$RV = \sum_{s=1}^{N_s} \pi_s \sum_{t=1}^{T} \sum_{l=1}^{L} \lambda_t^L \left(P_{l,t,s} \right) + \sum_{t=1}^{T} \lambda_t^N P_{t,s}^N \qquad s = 1, 2, ..., N_s \tag{6}$$

where λ_t^L is power market price that consumers pay at t^{th} time, $P_{l,t,s}$ is active power demand of l^{th} load at t^{th} time in s^{th} scenario, $P_{t,s}^N$ is power sold to the upstream network at t^{th} time and s^{th} scenario, λ_t^N is price of selling /purchasing power to/ from the upstream network at t^{th} time, t is index of time, n is index of dispatchable unit, l is index of load and s is index of scenarios. π_s is the probability of scenario s.

The total operation cost for MG's owner includes fuel cost, start-up and shut-down cost, emission cost of dispatchable units, cost of purchasing power from the upstream network and switching cost that is calculated as follows:

$$TC = \sum_{s=1}^{N_s} \pi_s \sum_{n=1}^{N} \sum_{t=1}^{T} (F(P_{n,t,s}) X_{n,t,s} + SU_{n,t,s} + SD_{n,t,s} + (C_n^{em}.\tau_n.P_{n,t,s})) + \sum_{t=1}^{T} \lambda_t^N P_{t,s}^b + \sum_{t=1}^{T} \sum_{j=1}^{N_j} N_{j,t}^{sw} \lambda^{sw} \quad (7)$$

Where $X_{n,t,s}$ is the commitment state of the n^{th} MT at the t^{th} time interval and scenario *s*. $F(P_{n,t,s})$ is fuel cost consumption function of the n^{th} micro-turbine at t^{th} time and scenario *s* that is calculated as follows:

$$F(P_{n,t,s}) = a_n + b_n P_{n,t,s} + c_n (P_{n,t,s})^2 \qquad \text{n} \in N,\ t \in T \quad (8)$$

In (8), a_n, b_n and c_n are cost coefficients of the n^{th} MT, $P_{n,t,s}$ is power output of the n^{th} MT at the t^{th} time and scenario *s*.

The second and the third terms of (7), represent start-up and shut-down cost, respectively. The fourth term represents the emission cost of the n^{th} MT, τ_n is emission factor *(kg/kWh)* of the n^{th} MT and C_n^{em} is emission cost of the n^{th} MT *($/kg)* [33]. The fifth term represents the price of purchased power and $P_{t,s}^b$ is purchased power from the upstream network at the t^{th} time interval and scenario *s*. The last term of (7), represents switching cost which is caused by the RG process, λ^{sw} is the cost of each switching action for switches, and $N_{j,t}^{sw}$ is a number of switching action of the j^{th} switch at the t^{th} time interval. The state of each switch can be 0 and 1 which show the open or closed state of switch, therefore, N_j^{sw} at the t^{th} time can be calculated as:

$$N_j^{sw} = \sum_{t=1}^{T} \left| S_{j,t} - S_{j,t-1} \right| \quad (9)$$

In (9), $S_{j,t}$ and $S_{j,t-1}$ are state of the j^{th} switch at the t^{th} and $t\text{-}1^{th}$ time intervals, respectively.

3.1. Problem constraints

3.1.1. Power balance constraint: The sum of generated power by dispatchable units (MTs and ESS) and non-dispatchable units (PV and WT) and exchanged power with the upstream network must be greater or equal to the sum of the forecasted power demand and power loss as follows:

$$\sum_{n=1}^{N} P_{n,t,s}.X_{n,t,s} + P_{dis,s}(t)X^{d}_{t,s} - P_{char,s}(t)X^{c}_{t,s} + P_{PV,s}(t) + P_{WT,s}(t) + P_{grid,t,s} \geq P_{loss,t,s} + \sum_{l=1}^{L} P_{l,t,s} \qquad \begin{matrix} t \in T \\ s \in N_s \end{matrix} \qquad (10)$$

where $P_{dis,s}(t)$ / $P_{char,s}(t)$ and $X^{c}_{t,s}$ / $X^{d}_{t,s}$ are the charged/discharged power and the commitment state at the t^{th} time interval and scenario *s*, respectively. $X^{d}_{t,s}$ and $X^{c}_{t,s}$ are binary variables denoting the discharging and charging mode, respectively. $P_{PV,s}(t)$ is generated power by the PV at t^{th} time and scenario *s*, $P_{WT,s}(t)$ is generated power by the WT at the t^{th} time and scenario *s*; $P_{grid,t,s}$ is the exchanged power with the upstream network at t^{th} time and scenario *s*, if the power sold to the upstream network, $P_{grid,t,s} = P^{N}_{t,s}$, otherwise, $P_{grid,t,s} = P^{b}_{t,s}$ and power purchased from the upstream network. $P_{loss,t,s}$ is total power loss at the t^{th} time interval and scenario *s*.

3.1.2. Inequality constraints*:* The generated power by MTs and exchanged power are bounded by upper and lower limits as follows:

$$P_n^{\min} X_{n,t,s} \leq P_{n,t,s} \leq P_n^{\max} X_{n,t,s} \qquad t \in T \qquad (11)$$

$$P_{grid}^{\min} \leq P_{grid,t,s} \leq P_{grid}^{\max} \qquad t \in T \qquad (12)$$

where $P_n^{\min}$ and $P_n^{\max}$ are the minimum and maximum power output of the n^{th} MT, $P_{grid}^{\min}$ and $P_{grid}^{\max}$ are minimum and maximum exchanged power with the upstream network.

3.1.3. Energy storage constraint*:* The charging/discharging power of an ESS is bounded by upper and lower limits as follows:

$$P_{dis}^{\min} X_{t,s}^{d} \le P_{dis,s}(t) \le P_{dis}^{\max} X_{t,s}^{d} \qquad \forall t \in T \tag{13}$$

$$P_{char}^{\min} X_{t,s}^{c} \le P_{char,s}(t) \le P_{char}^{\max} X_{t,s}^{c} \qquad \forall t \in T \tag{14}$$

where $P_{dis}^{\min}$ and $P_{char}^{\min}$ are the minimum discharging and charging power, respectively. Similarly, $P_{dis}^{\max}$ ($P_{char}^{\max}$) shows the maximum discharging (charging) power. $X_{t,s}^{d}$ and $X_{t,s}^{c}$ are also binary variables for discharging and charging modes in scenario *s*. When charging, the variable $X_{t,s}^{c}$ is set to one while $X_{t,s}^{d}$ is kept as zero. The opposite happens if the battery is switched into discharging mode. To distinguish the ESS operation modes (ESS cannot operate in both charging and discharging modes, simultaneously), another constraint is considered as follows:

$$X_{t,s}^{c} + X_{t,s}^{d} \le 1 \qquad \forall t \in T \tag{15}$$

Constraint (16) calculate the current SOC that is function of amount of charging and discharging level at current time and level of SOC at the previous time [34]. η^{char} and η^{dis} are charge and discharge efficiency, respectively. It is also assumed that energy storage systems maintain similar SOC at the beginning and end of the scheduling horizon (constraint 17). Energy storage system state of charge (SOC) is limited by maximum value which is shown in (18):

$$SOC_{t+1,s} = SOC_{t,s} + \eta^{char} P_{char,s}(t) - \frac{P_{dis,s}(t)}{\eta^{dis}} \tag{16}$$

$$SOC_{0} = SOC_{24} \tag{17}$$

$$SOC^{\min} \le SOC_{t,s} \le SOC^{\max} \qquad \forall t \in T \tag{18}$$

where $SOC^{\max}$ is maximum state of charge, $E^{\max}$ is maximum ESS capacity (kWh). Energy storage system should follow charging and discharging time limits, respectively:

$$\begin{aligned} T^{char} &\ge MC_{e}\left(X_{t,s}^{c} - X_{t-1,s}^{c}\right) \\ T^{dis} &\ge MD_{e}\left(X_{t,s}^{d} - X_{t-1,s}^{d}\right) \end{aligned} \qquad \forall t \in T \tag{19}$$

where MC_e and MD_e are the minimum charging and discharging time of the e^{th} ESS, respectively. T^{char} and T^{dis} are the number of continuous charging and discharging time (per hour).

***3.1.4. Minimum up and down time**:* A dispatchable unit must be on/off for a certain time before it can be start-up or shut-down again, respectively [35]:

$$\begin{aligned} &MUT_n\left(X_{n,t,s}-X_{n,t-1,s}\right)\le T_n^{on} \\ &MDT_n\left(X_{n,t-1,s}-X_{n,t,s}\right)\le T_n^{off} \end{aligned} \tag{20}$$

where MUT_n and MDT_n are the minimum up and down-time of the n^{th} MT, $X_{n,s}$ and $X_{n,t-1,s}$ are commitment state of the n^{th} MT at the $t\text{-}1^{th}$ and the t^{th} time intervals and scenario s, respectively. T_n^{on} and T_n^{off} are numbers of hours that the n^{th} MT is on and off, respectively.

3.1.5. Start-up / Shut-down constraint: The second and the third terms of (7) which represent the start-up and shut-down costs of generating units are enforced by constraints (21) and (22) as following [36, 37]:

$$\begin{aligned} &STU_n\left(X_{n,t,s}-X_{n,t-1,s}\right)\le SU_{n,t,s} \\ &SU_{n,t,s}\ge 0 \end{aligned} \tag{21}$$

$$\begin{aligned} &STD_n\left(X_{n,t-1,s}-X_{n,t,s}\right)\le SD_{n,t,s} \\ &SD_{n,t,s}\ge 0 \end{aligned} \tag{22}$$

Where STU_n and STD_n are start-up and shut-down coefficient of n^{th} MT.

3.1.6. Node voltage constraint: Bus voltage must be in an acceptable range:

$$V_b^{\min}\le V_b\le V_b^{\max} \tag{23}$$

where $V_b^{\min}$ and $V_b^{\max}$ are minimum and maximum voltage ranges of the b^{th} bus.

***3.1.7. Brunch current constraint**:* The value of current of the j^{th} branch should be less than the maximum allowable current range as follows:

$$\left|I_j\right| \le I_j^{\max} \tag{24}$$

It should be noted that the microgrid daily scheduling considering reconfiguration capability associated with AC optimal power flow (AC-OPF). All the AC-OPF calculation is done by MATPWER toolbox in MATLAB software based on Newton-Raphson method [38].

3.1.8. Radial topology constraint*:* The proposed RG model will be implemented on a radial MG, so after the determination of the optimal structure for each hour, MG's topology should not include any rings. Radial operation condition of the networks is established as following:

$$\sum_{j \in \phi_b^{in}} N_{j,b}^{sw} \le 1 \tag{25}$$

Between two buses, the line is represented by double direction of the power flow. In the operation of the networks, only one of the directions should exist [39, 40]. In (25), $N_{j,b}^{sw}$ is decision variable to connect line *j* to node *b* and ϕ_b^{in} is subset of lines that enter node b. In order to maintain the radiality of the system, the number of closed lines in each loop needs to be less than the total number of lines making the loop as prescribed by (25).

3.1.9. Maximum number of switching action*:* Another constraint is considered to limit the maximum number of switching action during the RG process as follows:

$$N_j^{sw} \le N^{sw,\max} \tag{26}$$

where $N^{sw,\max}$ is the maximum number of switching action during the day.

3.2. Decision variables

It is observed that profit-based maximization of RMG problem has various variables contains binary variables (i.e., $X_{n,t,s}$,$X_{e,t,s}$ and $S_{j,t}$), and real variables (i.e. $P_{n,t,s}$, $P_{dis/char_{N_e},t}$, $P_{loss,t,s}$ and

$P_{grid,t,s}$). In the examined MG which is described in the following, there are N MTs, N_e ESSs and N_{sw} switches, therefore, the state of these variables are considered as decision variables. Hence, there are multiple decision variables for each hour that must be determined. All decision variables for day-ahead can be represented by a matrix as follow (It should be noted that the scenario index *s* is ignored to reduce the volume of equation):

$$\begin{bmatrix} \overbrace{X_{1,1} \ \cdots \ X_{N,1}}^{MT\ state} & \overbrace{P_{1,1} \ \cdots \ P_{N,1}}^{MT\ output} & \overbrace{X_{1,1} \ \cdots \ X_{N_e,1}}^{ESS\ state} & \overbrace{P_{dis/char_{1,1}} \ \cdots \ P_{dis/char_{N_e,1}}}^{ESS\ char/dis} & P_{grid} & P_{loss} & \overbrace{S_{1,1} \ S_{2,1} \ \cdots \ S_{N_{sw},1}}^{Switch\ status} \\ \vdots \ \vdots & \vdots \ \vdots & \vdots \ \vdots & \vdots \ \vdots & \vdots & \vdots & \vdots \ \vdots \ \vdots \\ \vdots \ \vdots & \vdots \ \vdots & \vdots \ \vdots & \vdots \ \vdots & \vdots & \vdots & \vdots \ \vdots \ \vdots \\ X_{1,23} \ \cdots \ X_{N,23} & P_{1,23} \ \cdots \ P_{N,23} & X_{1,23} \ \cdots \ X_{N_e,24} & P_{dis/char_{1,23}} \ \cdots \ P_{dis/char_{N_e,23}} & P_{grid,23} & P_{loss,23} & S_{1,23} \ S_{2,23} \ \cdots \ S_{N_{sw},23} \\ X_{1,24} \ \cdots \ X_{N,24} & P_{1,24} \ \cdots \ P_{N,24} & X_{1,24} \ \cdots \ X_{N_e,24} & P_{dis/char_{1,24}} \ \cdots \ P_{dis/char_{N_e,24}} & P_{grid,24} & P_{loss,24} & S_{1,24} \ S_{2,24} \ \cdots \ S_{N_{sw},24} \end{bmatrix} \quad (27)$$

The number of rows and columns of this matrix demonstrate the scheduling horizon and decision variables, respectively.

4. Solution method

As mentioned before, to find the optimal configuration of RMG, the TVAC-PSO algorithm is used. In this section, the details of the TVAC-PSO algorithm and its implementation in profit-based RMG scheduling problem are described.

4.1. TVAC-PSO approach

PSO is one of the commonly used heuristic techniques for the power system optimization problem. In the conventional PSO, each particle moves toward the best position in appointed speed. Let χ_p and υ_p denote the p^{th} particle's position and velocity, respectively. In the n-dimensional search space, velocity and position vector of the p^{th} particle is represented as $\upsilon_p = (\upsilon_{p1}, \upsilon_{p2}, \ldots, \upsilon_{pn})$ and $\chi_p = (\chi_{p1}, \chi_{p2}, \ldots, \chi_{pn})$, respectively. The best position of the p^{th} particle in previous iterations is stored and demonstrated by

P_{best}. The best particle among all particles is represented by the G_{best} [41]. The new velocity and position of the p^{th} particle can be formulated as:

$$\upsilon_p(t+1) = \omega \times \upsilon_p(t) + C_1 \times rand_1 \times \left(P_{best} - \chi_p(t)\right) + C_2 \times rand_2 \times \left(G_{best} - \chi_p(t)\right) \quad (28)$$

$$\chi_p(t+1) = \chi_p(t) + \upsilon_p(t+1) \quad (29)$$

where:

$\upsilon_p(t+1)$: is modified velocity of the p^{th} particle at the $t+1^{th}$ time interval.

$\upsilon_p(t)$: is current velocity of the p^{th} particle at the t^{th} time interval.

C_1 and C_2 : are the acceleration coefficients.

$rand_1$ and $rand_2$: are random numbers.

$\chi_p(t+1)$: is modified position of the p^{th} particle at the $t+1^{th}$ time interval.

$\chi_p(t)$: is current position of the p^{th} particle at the t^{th} time interval.

ω : is inertia weight, which is formulated as:

$$\omega = \omega_{\min} + \frac{Iter_{\max} - Iter}{Iter_{\max}} \left(\omega_{\max} - \omega_{\min}\right) \quad (30)$$

where:

$Iter_{\max}$: is maximum number of iterations.

$Iter$: is current iteration number.

$\omega_{\min}$ and $\omega_{\max}$: are minimum and maximum inertia weight.

It has been demonstrated by many researchers that tuning of parameters is a key factor in the PSO algorithm to have a better performance. For example, by changing the acceleration coefficients (C_1 and C_2) along the algorithm iterations, better exploitation can be achieved [41]. The convergence and solution quality of PSO is affected by selection of the acceleration coefficients. The relatively high

value of the social component (C_2) comparing with cognitive component (C_1) leads particles to local optimum prematurely and relatively high values of cognitive components results to wander the particles around the search space [8, 42, 43]. The acceleration coefficients are fixed values in classic PSO. To improve the solution quality, these coefficients are updated in a way that the cognitive component is reduced and social component is increased as iteration proceeds.

So, unlike the conventional PSO, the acceleration coefficients are updated in this work as follows:

$$C_1 = c_{1i} + \frac{Iter}{Iter_{\max}}(c_{1f} - c_{1i}) \tag{31}$$

$$C_2 = c_{2i} + \frac{Iter}{Iter_{\max}}(c_{2f} - c_{2i}) \tag{32}$$

4.2. The implementation of TVAC-PSO in RMG profit-based scheduling

In this section, the implementation of TVAC-PSO for the day-ahead profit-based RMG scheduling problem is presented. The procedure of implementation the proposed TVAC-PSO approach is shown in Fig. 4. The steps of the proposed method for profit-based RMG optimal scheduling using RG and UC by the TVAC-PSO algorithm are as follows:

At first, the initial data consists of MT's cost and emission coefficients, line data, switches status etc., are considered as input data. By using the uncertainty modeling in section 2 based on MCS and LHS technique consider the autocorrelation model for PV and wind power output, a number of scenario for wind, PV and load demand are generated. Therefore, the current scenario consists of a 1×24 vector for wind, 1×24 vector for PV and L×24 matrix for day-ahead load demand. In the next step, decision variables based on TVAC-PSO algorithm are generated for 24-h period considering their limitations. All decision variables of day-ahead ($P_{n,t}$, $X_{n,t}$, $P_{dis/char_{N_e},t}$, X_t^c, X_t^d, $S_{j,t}$) are optimized, simultaneously. After that power loss is determined by AC power flow calculation by MATPOWER and all of the problem constraints are checked for each hour. As the TVAC-PSO

algorithm iterations reach maximum value, the optimal set point of MTs (commitment state and power output), power exchange, charging/ discharging of ESS and RMG's topology are determined for the current scenario. After enough scenario generation $Iter = Iter_{\max}$, the value of objective function (daily benefit), MTs power output, power exchange, ESS status, and etc., for each hour are determined by scenario aggregation. Finally, If $Scen.num=N_s$ the algorithm is stopped and the expected value for each variable is calculated. It should be noted that the average value of continuous variables and most repeated discrete variables for each hour are determined for the next day. Also the expected value of profit for the day based on solution of each scenario and its probability ($\sum_{s=1}^{N_s} \pi_s Profit_s$) is calculated.

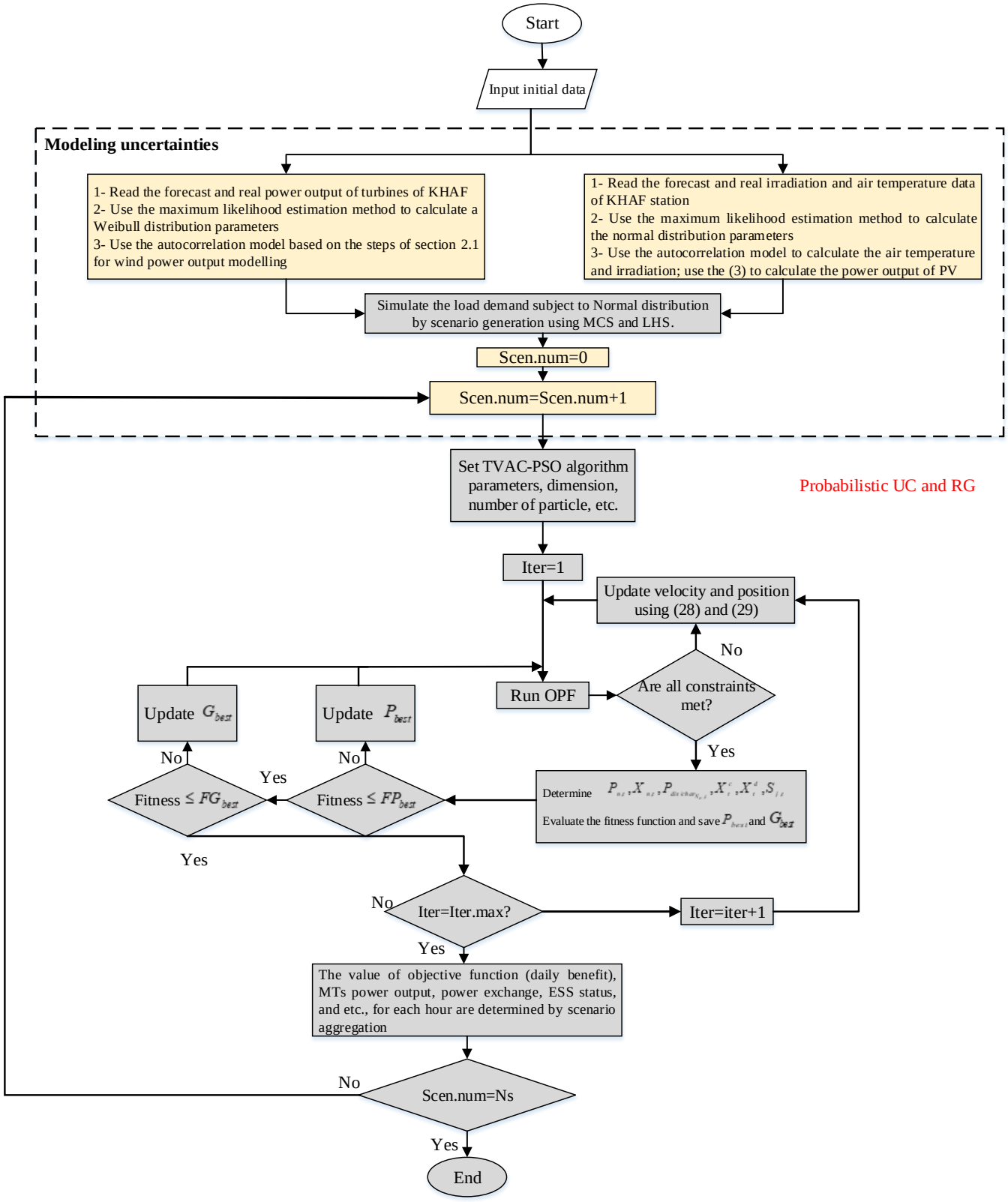

Fig. 4. The flowchart of the proposed algorithm.

5. Simulation results

The proposed solution method, which was presented in the previous section, is implemented on a 69-bus radial MG test system. This test system consists of MTs, PVs, WTs, ESSs, different loads and five normally opened switches. The schematic of the test system is shown in Fig. 5. The characteristics of MTs are given in Table 1.

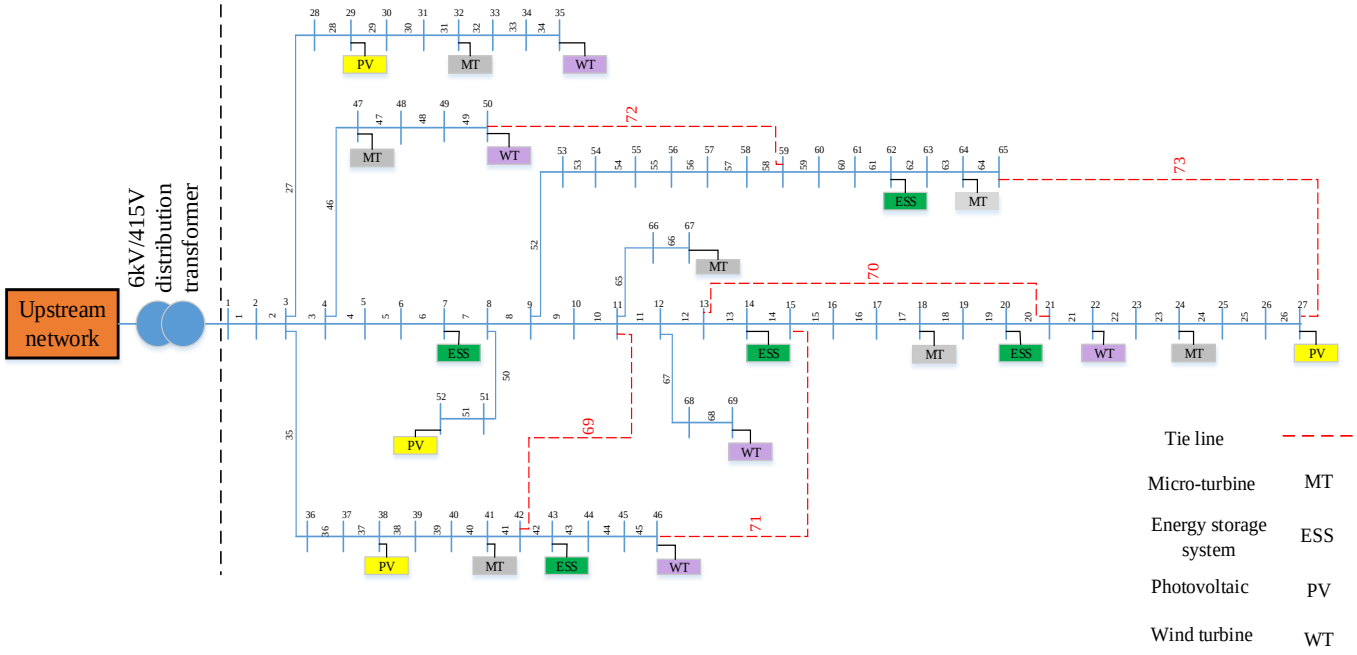

Fig. 5. The single line diagram of 69-Bus radial system

Table 1. Micro-turbine characteristics

MT	MT1	MT2	MT3	MT4	MT5	MT6	MT7
Bus	32	41	47	67	64	18	24
$P_{\min}$ (kW)	25	50	75	75	50	25	50
$P_{\max}$ (kW)	300	200	150	150	200	300	250
a	25	15	10	10	12	20	18
b	0.045	0.104	0.12	0.12	0.08	0.085	0.09
c	0.002	0.007	0.01	0.01	0.008	0.003	0.003
Star-tup/Shut down cost($)	0.096	0.102	0.19	0.19	0.14	0.096	0.102

The characteristics of ESS are given in Table 2. Table 3 and Table 4 show the values of parameters of PV and WT and their bus number where they are located, respectively. The parameters of TVAC-

PSO are given in Table 5. The expected value of load demand during all time periods will be employed as the basic data, as shown in Fig. 6.

Table 2. Energy storage characteristic

	ES1	ES2	ES3	ES4	ES5
BUS	43	7	62	14	20
Min/max charge or discharge power (kw)	-50/+50	-50/+50	-40/+40	-40/+40	-40/+40
Capacity (kWh)	100	150	80	80	120

Table 3. PV characteristics

	T_c	P_{STC}	G_{STC}	K	BUS
PV	$25\,^{o}C$	250 kW	$1000W/m^2$	0.001	29,38,52,27

Table 4. Wind turbine characteristics

	V_{cut-in}	$V_{cut-out}$	V_{rated}	$P_{wind}^{\min}$	$P_{wind}^{\max}$	BUS
WT	3	25	12	0	100	35,50,46, 69, 22

Table 5. TVAC-PSO parameters

Parameter	value
Maximum iteration number	50
Population size	2640
$\omega_{\min}$	0.4
$\omega_{\max}$	0.9

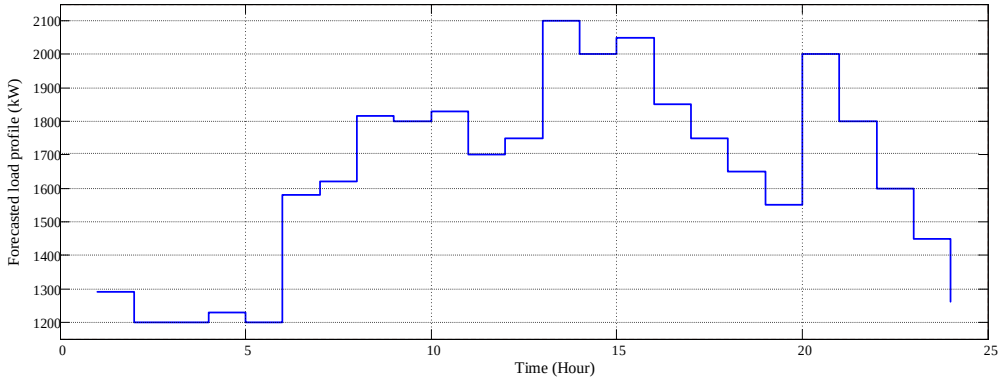

Fig. 6. The average value of load demand scenarios.

The maximum number of switching action for each switch is considered as 10 actions during the day. Also, the cost of each switching action is $1 [44].The value of emission factor and emission cost are fixed at 0.003 *kg/kWh* and 0.02 *$/kg*, respectively [33]. Computer simulations and required coding are carried out in MATLAB software. Fig. 7 shows the convergance curve of the fitness function. As can be seen, the algorithm converged in iteration number 23.

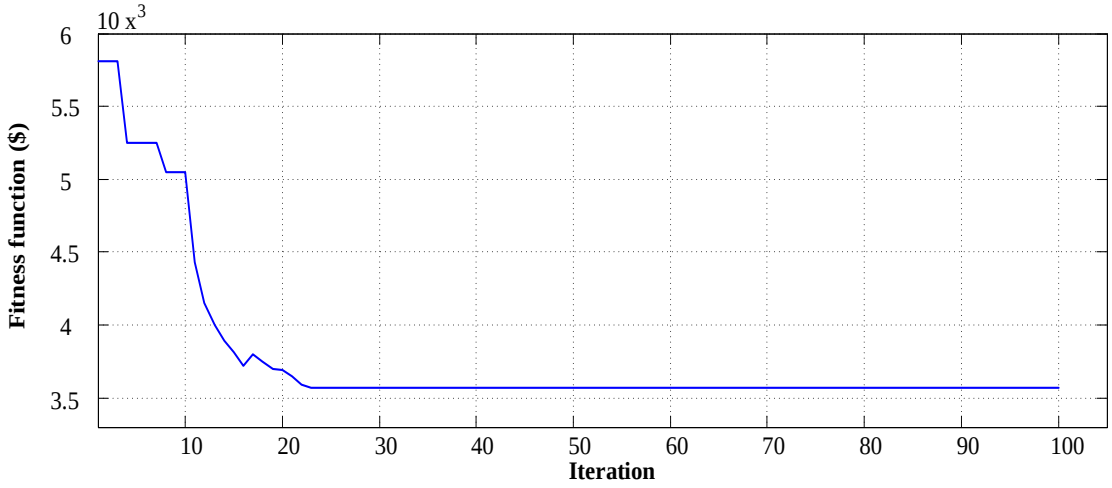

Fig. 7. The convergence curve of TVAC-PSO algorithm.

To examine the effect of RG and UC in profit-based MG optimal scheduling problem, two cases are considered. For Case 1, the optimal MG scheduling and profit maximization problem is solved by using UC. For Case 2, the intended problem is solved for simultaneous RG and UC. The value of the objective function is calculated and compared with two cases.

Case1: In this case, profit-based RMG optimal scheduling is solved by using UC while RG is neglected. Based on daily power market price and exchanged power price that are shown in Table 6, the proposed algorithm finds the decision variables $(X_{i,t}, X_{e,t}, S_{j,t})$.

Table 6. Hourly energy price [10]

Hour	Power exchanged price ($/kwh)	Power market price ($/kwh)
1	0.06	0.11
2	0.06	0.11
3	0.06	0.11

4	0.06	0.11
5	0.06	0.11
6	0.06	0.11
7	0.06	0.11
8	0.06	0.11
9	0.09	0.13
10	0.09	0.13
11	0.09	0.13
12	0.12	0.13
13	0.145	0.17
14	0.16	0.17
15	0.17	0.195
16	0.175	0.18
17	0.17	0.18
18	0.14	0.16
19	0.1	0.13
20	0.08	0.13
21	0.08	0.125
22	0.08	0.13
23	0.07	0.12
24	0.06	0.11

The monetary results of the problem in terms of RMG's costs, revenues and profits are given in Table 7, for Case1.

Table 7. Dispatch scheduled and monetary value for Case 1

	Power dispatch (kW)							Monetary value				
Hour	**MT1**	**MT2**	**MT3**	**MT4**	**MT5**	**MT6**	**MT7**	**Gen cost($)***	**Emission cost($)**	**Energy import cost($)**	**Total revenue($)**	**Profit**
1	300	0	0	0	0	250	0	62.8	7.92	24.6	141.9	46.58
2	300	0	0	0	0	250	0	62.8	7.92	25.2	132	36.08
3	300	0	0	0	0	250	0	62.8	7.92	25.2	132	36.08
4	300	0	0	0	0	250	0	62.8	7.92	29.88	135.3	34.7
5	300	0	0	0	0	250	0	62.8	7.92	24.18	132	37.1
6	300	0	0	0	0	250	0	62.8	7.92	46.5	173.8	56.58
7	300	0	0	0	0	250	0	62.8	7.92	35.7	178.2	71.78
8	300	0	0	0	0	250	150	85.375	10.08	54	235.95	86.495
9	300	0	0	0	0	300	200	95.7	11.52	41.58	234	85.2
10	300	50	0	0	0	300	250	118.875	12.96	23.4	237.9	82.665
11	300	150	0	0	75	300	250	130.575	15.48	0	256	109.945
12	300	200	0	0	150	300	250	145.875	17.28	0	330.415	167.26
13	300	200	100	0	200	300	250	182.375	19.44	0	397	195.185
14	300	200	150	125	200	300	250	286.75	21.96	0	460.4	151.69
15	300	200	150	125	200	300	250	256.75	21.96	0	443.3.75	164.665
16	300	200	75	0	200	300	250	160	19.08	0	379.75	200.67
17	300	200	0	0	0	300	250	145.875	15.12	0	284.2	123.205
18	300	0	0	0	0	300	250	105.975	12.24	8.3	214.5	87.985
19	300	0	0	0	0	300	250	105.975	12.24	6.64	201.5	76.645
20	300	150	0	0	120	300	250	138.075	16.128	23.84	250	71.957
21	300	150	0	0	50	300	200	120.3	14.4	35.2	234	64.1
22	300	50	0	0	0	300	120	88.716	11.088	29.4	192	62.796
23	300	0	0	0	0	250	120	73.816	9.648	32.25	159.5	43.786
24	300	0	0	0	0	250	0	62.8	7.92	21	138.6	46.88
									Total cost ($)			
									3534.261		**5674.29**	**2140.029**

It is seen from Table 7, at the peak load hours (11:00-16:00) when the electricity market price exceeds MTs marginal cost, MG's owner sells surplus power (through dispatching more MTs) to the upstream network and get a significant revenue.

Based on the proposed optimal scheduling, the profit of the MG owner is determined as $ 2140.029 The value of power loss for Case1 is around 3737.24 kWh.

The optimal MTs and ESSs state for 24-h are given in Table 8 and 9, respectively. ESS charging, discharging and idle states are represented by -1, 1 and 0, respectively. As can be seen from Table 1, MTs number 3 and 4 are high-cost MT, so they are committed in peak-load hours (13- to 16-hour).

The proposed algorithm detects that price of exchanged power is low at some hours (1- to 8-hour), so purchasing power from the upstream network is beneficial for MG's owner. In this interval, most of ESSs are charged. As the exchanged power price rises (at 8:00), the MT number 7 is committed beside MT number 1 and 6 (MTs number 1 and 6 are dispatched during the entire scheduling horizon). At the higher exchanged power price (during 10:00 to 16:00), it is beneficial for MG owner to sell surplus power to the upstream network and make a significant benefit. In this interval, most of ESSs are discharged and due to the higher cost of exchanged energy compared to the cost of dispatchable units within the MG, MTs number 2 and 5 are dispatched at 10:00 and 11:00, respectively, and MTs number 3 and 5 are dispatched thereafter. While MG supplying its loads, surplus power is sold to the upstream network.

Table 8. MTs scheduling based on decision variables in Case 1

H	1	2	3	4	5	6	7	8	9	10	11	12	13	14	15	16	17	18	19	20	21	22	23	24
MT1	1	1	1	1	1	1	1	1	1	1	1	1	1	1	1	1	1	1	1	1	1	1	1	1
MT2	0	0	0	0	0	0	0	0	0	1	1	1	1	1	1	1	1	0	0	1	1	1	0	0
MT3	0	0	0	0	0	0	0	0	0	0	0	0	1	1	1	1	1	0	0	0	0	0	0	0
MT4	0	0	0	0	0	0	0	0	0	0	0	0	0	1	1	0	0	0	0	0	0	0	0	0
MT5	0	0	0	0	0	0	0	0	0	0	1	1	1	1	1	1	0	0	0	1	1	0	0	0
MT6	1	1	1	1	1	1	1	1	1	1	1	1	1	1	1	1	1	1	1	1	1	1	1	1
MT7	0	0	0	0	0	0	0	1	1	1	1	1	1	1	1	1	1	1	1	1	1	1	1	0

Table 9. Optimal 5-ESS scheduling based on decision variables in Case 1

H	1	2	3	4	5	6	7	8	9	10	11	12	13	14	15	16	17	18	19	20	21	22	23	24
ES1	-1	-1	-1	-1	-1	-1	0	0	0	1	1	1	1	0	0	0	0	1	1	1	0	0	0	0
ES2	-1	-1	-1	-1	-1	-1	0	0	0	0	1	1	1	1	0	0	0	0	1	1	1	0	0	0
ES3	-1	-1	-1	-1	0	0	0	0	0	0	0	0	1	1	1	1	0	0	0	0	0	0	0	0
ES4	0	0	0	-1	-1	-1	-1	0	0	0	1	1	1	0	0	1	1	1	0	0	0	0	0	0
ES5	0	0	0	0	-1	-1	-1	-1	-1	0	0	0	1	1	1	1	0	0	0	0	0	0	0	0

It should be noted that the schematic of test system is shown in Fig. 5 is default configuration, that means switches number 69-73 are opened along the day.

C**ase2:** As previously discussed, in this case, RG and UC techniques are implemented on profit maximization problem, simultaneously. Similar to Case 1, we execute ten profit-based optimal scheduling and describe one of them in detail.

The 69-bus MG test system shown in Fig. 5, has 73 switches, 68 normally-closed switches (switches number 1-68) and five normally-opened switches (switches number 69-73). MG can have various structures during the day, however each topology which is obtained by the proposed method must meet radial structure constraint. Therefore, at any hour, five switches must be opened. The changes in MG's topology will change the power flow direction in lines and power loss, so power dispatch and unit states will be changed, subsequently. Hence, it is expected that utilization of simultaneous RG process and UC, could result in utilization of maximum available power capacity and prevents the commitment of additional MTs. The proposed method finds the optimal state of decision variables. At any hour, TVAC-PSO determines 85 decision variables: 7 binary variables for MTs commitment state ($x_{i,t}$), five binary variables for ESSs commitment state ($x_{e,t}$), and 73 binary variables for switches status which describe the MG's topology at the current hour ($s_{i,t}$). The optimal MG structure is determined from profit maximization point of view. Table 10 shows the optimal results of RG process at any hour for Case 2. There are five opened switches at any hour which their

numbers are given in Table 10. According to MG's topology, MTs and ESSs commitment state are changed in comparison with Case 1.

Table 10. Optimal result of hourly reconfiguration process

Hour	Switches opened	Hour	Switches opened
1	14- 56- 61- 69- 70	**13**	10- 14- 16- 55- 62
2	12- 58- 61- 69- 70	**14**	10- 14- 16- 55- 62
3	12- 58- 61- 69- 70	**15**	10- 14- 16- 55- 62
4	13- 18- 56- 61- 69	**16**	10- 14- 16- 55- 62
5	14- 56- 61- 69- 70	**17**	10- 15- 45- 55- 61
6	13- 57- 63- 69- 70	**18**	10- 15- 45- 55- 61
7	13- 18- 56- 61- 69	**19**	13- 17- 55- 61- 69
8	13- 17- 55- 61- 69	**20**	10- 15- 45- 55- 61
9	14- 56- 61- 69- 70	**21**	10- 15- 45- 55- 61
10	14- 56- 61- 69- 70	**22**	12- 56- 61- 69- 70
11	14- 56- 61- 69- 70	**23**	12- 56- 61- 69- 70
12	10- 14- 16- 55- 62	**24**	12- 56- 61- 69- 70

The monetary result of problem consists of MG's costs, revenues and profits based on MG's topology, are given in Table 11, for Case2. As can be seen from Table 11, MTs number 3 and 4 are not committed during the scheduling horizon. MTs 2, 5 and 7 are committed less than in the previous case study. Compared to Case1, the number of hours that MG purchases power is less.

Table 11. Dispatch scheduled and monetary value for Case 2

	Power dispatch (kW)							Monetary value				
Hour	**MT1**	**MT2**	**MT3**	**MT4**	**MT5**	**MT6**	**MT7**	**Gen cost($)***	**Emission cost($)**	**Energy import cost($)**	**Total revenue($)**	**Profit**
1	300	0	0	0	0	170.61	0	50.7984	6.7768	28.11	141.9	56.21
2	300	0	0	0	0	94.36	0	42.8301	5.6787	30.024	132	53.4672
3	300	0	0	0	0	144.82	0	47.7123	6.4054	29.0016	132	48.88
4	300	0	0	0	0	224.87	0	58.5923	7.5581	27.15	135.3	42
5	300	0	0	0	0	166.76	0	50.3117	6.7213	24.1602	132	50.8068
6	300	0	0	0	0	250	0	62.8	7.92	40.4055	173.8	62.674
7	300	0	0	0	0	132.36	0	46.3654	6.226	35.4396	178.2	90.169
8	300	0	0	0	0	220	0	57.82	7.488	56.8926	235.95	113.75
9	300	0	0	0	0	200	0	54.8	7.2	51.0727	234	120.9273
10	300	0	0	0	0	300	200	103.2	11.52	18.2855	237.9	104.894
11	300	93.5	0	0	0	300	250	125.359	13.5864	0	256.648	117.702
12	300	193.5	0	0	0	300	250	143.671	15.0264	0	332.358	163.6606
13	300	200	0	0	112.96	300	250	145.875	16.7466	0	392.354	229.732
14	300	200	0	0	150	300	250	145.875	17.28	0	456.109	292.954
15	300	200	0	0	200	300	250	145.875	18	0	423.163	259.288
16	300	200	0	0	176.4	300	250	145.875	17.6601	0	383.424	220.88
17	300	175.5	0	0	0	300	250	137.903	14.7672	0	296.131	143.4608
18	300	0	0	0	0	300	204.24	96.4971	11.5811	2	214.5	104.4218
19	300	0	0	0	0	300	179.54	92.0585	11.2254	0	201.5	98.2161
20	300	93.5	0	0	0	300	250	125.359	13.5864	23.36	250	87.694
21	300	93.5	0	0	0	300	250	117.859	13.5864	18.12	234	84.435
22	300	0	0	0	0	300	150	87.375	10.8	27.3128	192	66.513
23	300	0	0	0	0	250	0	62.8	7.92	34.8033	159.5	53.977
24	300	0	0	0	0	191	0	53.5193	7.0704	24.15	138.6	53.861
									Total cost ($)			
									2933.75		**566333**	**2729.587**

The result of UC for MTs and ESSs in Case 2 are shown in Table 12 and 13, respectively.

As the previous case and based on power market price, for the profit maximization achievement, high-cost MTs are committed at peak load hours. MTs number 3 and 4 are not committed during scheduling horizon due to their high cost of operation, so MG's cost is reduced in comparison with Case1. According to Table 13, all ESSs are charged in the low-load hour (1:00 to 8:00), and are discharged at the peak-load hour (11:00 to 17:00). The highlighted cells in Table 12 and 13, demonstrate the hours in which the commitment states of MTs and ESSs are different from those in Case1.

Implementation of the proposed optimal MG scheduling using joint UC and RG actions, reduces RMG's costs to $ 2933.75. RMG's profit is also determined as $ 2729.587. The cost of switching during reconfiguration is $ 0.1. The total power loss is determined as 2130.23 kWh for Case2.

Table 12. MTs scheduling based on decision variables in Case 2

H	1	2	3	4	5	6	7	8	9	10	11	12	13	14	15	16	17	18	19	20	21	22	23	24
MT1	1	1	1	1	1	1	1	1	1	1	1	1	1	1	1	1	1	1	1	1	1	1	1	1
MT2	0	0	0	0	0	0	0	0	0	**0**	1	1	1	1	1	1	1	0	0	1	1	**0**	0	0
MT3	0	0	0	0	0	0	0	0	0	0	0	0	**0**	**0**	**0**	**0**	**0**	0	0	0	0	0	0	0
MT4	0	0	0	0	0	0	0	0	0	0	0	0	0	**0**	**0**	0	0	0	0	0	0	0	0	0
MT5	0	0	0	0	0	0	0	0	0	0	**0**	**0**	1	1	1	1	0	0	0	**0**	**0**	0	0	0
MT6	1	1	1	1	1	1	1	1	1	1	1	1	1	1	1	1	1	1	1	1	1	1	1	1
MT7	0	0	0	0	0	0	0	**0**	**0**	1	1	1	1	1	1	1	1	1	1	1	1	1	**0**	0

Table 13. Optimal 5-ESS scheduling based on decision variables in Case 2

H	1	2	3	4	5	6	7	8	9	10	11	12	13	14	15	16	17	18	19	20	21	22	23	24
ES1	-1	-1	-1	-1	-1	-1	0	0	**1**	1	1	1	1	0	0	0	0	1	1	1	0	0	0	0
ES2	-1	-1	-1	-1	-1	-1	0	0	0	0	1	1	1	1	0	0	0	0	1	1	1	0	0	0
ES3	-1	-1	-1	-1	**-1**	0	0	0	0	0	0	**1**	1	1	1	1	0	0	0	0	0	0	0	0
ES4	**-1**	**-1**	**-1**	-1	-1	-1	-1	0	0	0	1	1	1	**1**	0	1	1	1	0	0	0	0	0	0
ES5	**-1**	**-1**	**-1**	**-1**	-1	-1	-1	**0**	**1**	**1**	**1**	**1**	1	1	1	1	0	**1**	**1**	**1**	0	0	0	0

To demonstrate the superiority of the reconfiguration process for profit-based maximization problem, the results of Case1 and Case2 are compared in Table 14. The results tabulated in Table 12 show an improvement of 17 % in profit and 43 % in power losses per day by using UC and RG

actions. It can be seen that using RG can improve system total power loss and RMG's profit, significantly, without any extra costs. To express the effectiveness of the TVAC-PSO algorithm compared to the conventional PSO and the initial case without any algorithm, the comparison between the result of proposed method and exiting works in literature is done from power loss minimization point of view which is shown in Table 15.

Also, to illustrate the effect of reconfiguration in the scheduling of RMG, the amount of power exchanged with the upstream network for two cases are depicted in Fig. 8. As can be seen, RMG is taking advantage of the ability of reconfiguration, uses the maximum capacity to deliver local loads. Therefore, when the energy price is high (12-18 hour), RMG sells more power to the upstream network than Case 1 and gets more profits.

Table 14. Comparison of profit-based RMG scheduling solution by TVAC-PSO for various Cases

Method	Cost ($)	Improvement (%)	Power loss (kWh)	Improvement (%)
Case1	3534.261	——	3737.24	——
Case2	2933.75	16.991	2130.23	42.992

Table 15. The power loss result comparison for TAVAC-PSO, PSO and initial case in kWh.

Initial [45]	**Conventional PSO [46]**	**TVAC-PSO**
5398.9	2365.44	2130.23

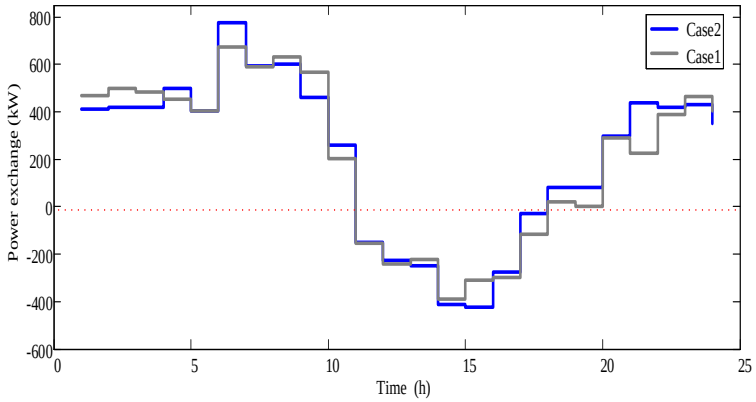

Fig. 8. The power exchanged between RMG and the upstream network for 2 cases

6. Conclusion

In this study, an optimal reconfigurable microgrid scheduling for day-ahead maximization profit in the presence of renewable energy resources (PV and Wind) and energy storage was presented. The uncertainties of renewable resources were modelled based on the autocorrelation model based on actual data of KHAF station, KHORASAN, IRAN. The uncertainty of load demand simulated by scenario generation using Monte Carlo and Latin Hypercube Sampling method with corresponding probability distribution functions. The commitment state of micro-turbines and energy storage systems together with switch status were considered as decision variables. A metaheuristic approach based on TVAC-PSO approach was proposed to solve the mentioned optimal scheduling problem. The MG's topology was determined from profit maximization point of view considering MTs and ESSs commitment state and exchanged power with the upstream network in each hour of day-ahead. The proposed approach was implemented on a 69-bus RMG test system and numerical results were reported for 2 cases: in Case1, optimal MG scheduling problem was solved using UC while neglecting RG action. In Case2, optimal scheduling problem for maximization RMG profit was solved using simultaneous RG and UC. Numerical results showed that in Case2, the value of day-ahead profit is 17 % higher than the one in Case1. Also, results of implementation of RG and UC in Case2, demonstrated that RMG's power loss could be decreased up to 43% compared to the case where there is no RG action.

References

[1] J. Shen, C. Jiang, Y. Liu, and X. Wang, "A Microgrid Energy Management System and Risk Management Under an Electricity Market Environment," *IEEE Access*, vol. 4, pp. 2349-2356, 2016.

[2] S. Parhizi, H. Lotfi, A. Khodaei, and S. Bahramirad, "State of the Art in Research on Microgrids: A Review," *Ieee Access*, vol. 3, pp. 890-925, 2015.

[3] M. Vahedipour-Dahraie, H. Rashidizadeh-Kermani, H. R. Najafi, A. Anvari-Moghaddam, and J. M. Guerrero, "Stochastic security and risk-constrained scheduling for an autonomous microgrid

with demand response and renewable energy resources," *IET Renewable Power Generation,* vol. 11, pp. 1812-1821, 2017.
[4] M.-A. Nasr, E. Nasr-Azadani, A. Rabiee, and S. H. Hosseinian, "Risk-averse energy management system for isolated microgrids considering generation and demand uncertainties based on information gap decision theory," *IET Renewable Power Generation,* 2019.
[5] S. Nikkhah, K. Jalilpoor, E. Kianmehr, and G. B. Gharehpetian, "Optimal wind turbine allocation and network reconfiguration for enhancing resiliency of system after major faults caused by natural disaster considering uncertainty," *IET Renewable Power Generation,* vol. 12, pp. 1413-1423, 2018.
[6] M. Horoufiany and R. Ghandehari, "Optimal fixed reconfiguration scheme for PV arrays power enhancement under mutual shading conditions," *IET Renewable Power Generation,* vol. 11, pp. 1456-1463, 2017.
[7] F. Shahnia, S. Bourbour, and A. Ghosh, "Coupling neighboring microgrids for overload management based on dynamic multicriteria decision-making," *IEEE Transactions on smart grid,* vol. 8, pp. 969-983, 2017.
[8] M. Hemmati, B. Mohammadi-Ivatloo, S. Ghasemzadeh, and E. Reihani, "Risk-based optimal scheduling of reconfigurable smart renewable energy based microgrids," *International Journal of Electrical Power & Energy Systems,* vol. 101, pp. 415-428, 2018.
[9] M. Hemmati, S. Ghasemzadeh, and B. Mohammadi-Ivatloo. (2019, Optimal scheduling of smart reconfigurable neighbour micro-grids. *IET Generation, Transmission & Distribution 13(3),* 380-389. Available: https://digital-library.theiet.org/content/journals/10.1049/iet-gtd.2018.6388
[10] R. Jabbari-Sabet, S.-M. Moghaddas-Tafreshi, and S.-S. Mirhoseini, "Microgrid operation and management using probabilistic reconfiguration and unit commitment," *International Journal of Electrical Power & Energy Systems,* vol. 75, pp. 328-336, 2016.
[11] S. Esmaeili, A. Anvari-Moghaddam, S. Jadid, and J. Guerrero, "A Stochastic Model Predictive Control Approach for Joint Operational Scheduling and Hourly Reconfiguration of Distribution Systems," *Energies,* vol. 11, p. 1884, 2018.
[12] M. H. Hemmatpour, M. Mohammadian, and A. A. Gharaveisi, "Optimum islanded microgrid reconfiguration based on maximization of system loadability and minimization of power losses," *International Journal of Electrical Power & Energy Systems,* vol. 78, pp. 343-355, 2016.
[13] X. Zhan, T. Xiang, H. Chen, B. Zhou, and Z. Yang, "Vulnerability assessment and reconfiguration of microgrid through search vector artificial physics optimization algorithm," *International Journal of Electrical Power & Energy Systems,* vol. 62, pp. 679-688, 2014.
[14] M. R. Ebrahimi and N. Amjady, "Adaptive robust optimization framework for day-ahead microgrid scheduling," *International Journal of Electrical Power & Energy Systems,* vol. 107, pp. 213-223, 2019.
[15] M. Bornapour, R.-A. Hooshmand, and M. Parastegari, "An efficient scenario-based stochastic programming method for optimal scheduling of CHP-PEMFC, WT, PV and hydrogen storage units in micro grids," *Renewable energy,* vol. 130, pp. 1049-1066, 2019.
[16] F. Yaprakdal, M. Baysal, and A. Anvari-Moghaddam, "Optimal Operational Scheduling of Reconfigurable Microgrids in Presence of Renewable Energy Sources," *Energies,* vol. 12, p. 1858, 2019.
[17] M. Hemmati, B. Mohammadi-Ivatloo, and A. Soroudi, "Uncertainty management in decision-making in power system operation," in *Decision Making Applications in Modern Power Systems,* ed: Elsevier, 2020, pp. 41-62.

[18] N. Nikmehr, S. Najafi-Ravadanegh, and A. Khodaei, "Probabilistic optimal scheduling of networked microgrids considering time-based demand response programs under uncertainty," *Applied energy,* vol. 198, pp. 267-279, 2017.
[19] F. S. Gazijahani and J. Salehi, "Robust Design of Microgrids with Reconfigurable Topology under Severe Uncertainty," *IEEE Transactions on Sustainable Energy,* 2017.
[20] G. Liu, M. Starke, B. Xiao, X. Zhang, and K. Tomsovic, "Microgrid optimal scheduling with chance-constrained islanding capability," *Electric Power Systems Research,* vol. 145, pp. 197-206, 2017.
[21] M. Javidsharifi, T. Niknam, J. Aghaei, and G. Mokryani, "Multi-objective short-term scheduling of a renewable-based microgrid in the presence of tidal resources and storage devices," *Applied Energy,* vol. 216, pp. 367-381, 2018.
[22] S. Nojavan, K. Zare, and B. Mohammadi-Ivatloo, "Optimal stochastic energy management of retailer based on selling price determination under smart grid environment in the presence of demand response program," *Applied Energy,* vol. 187, pp. 449-464, 2017.
[23] A. Mehdizadeh, N. Taghizadegan, and J. Salehi, "Risk-based energy management of renewable-based microgrid using information gap decision theory in the presence of peak load management," *Applied Energy,* vol. 211, pp. 617-630, 2018.
[24] F. S. Gazijahani and J. Salehi, "Integrated DR and reconfiguration scheduling for optimal operation of microgrids using Hong's point estimate method," *International Journal of Electrical Power & Energy Systems,* vol. 99, pp. 481-492, 2018.
[25] S. Mohammadi, S. Soleymani, and B. Mozafari, "Scenario-based stochastic operation management of microgrid including wind, photovoltaic, micro-turbine, fuel cell and energy storage devices," *International Journal of Electrical Power & Energy Systems,* vol. 54, pp. 525-535, 2014.
[26] A. Dolatabadi, B. Mohammadi-ivatloo, M. Abapour, and S. Tohidi, "Optimal stochastic design of wind integrated energy hub," *IEEE Transactions on Industrial Informatics,* vol. 13, pp. 2379-2388, 2017.
[27] Z.-S. Zhang, Y.-Z. Sun, J. Lin, L. Cheng, and G.-J. Li, "Versatile distribution of wind power output for a given forecast value," in *Power and Energy Society General Meeting, 2012 IEEE*, 2012, pp. 1-7.
[28] http://suna.org.ir/ationoffice-windenergyoffice-windamar-fa.html.
[29] X. Dui, G. Zhu, and L. Yao, "Two-stage optimization of battery energy storage capacity to decrease wind power curtailment in grid-connected wind farms," *IEEE Transactions on Power Systems,* vol. 33, pp. 3296-3305, 2018.
[30] Y. Chen, J. Wen, and S. Cheng, "Probabilistic load flow method based on Nataf transformation and Latin hypercube sampling," *IEEE Transactions on Sustainable Energy,* vol. 4, pp. 294-301, 2013.
[31] J. Wang, M. Shahidehpour, and Z. Li, "Security-constrained unit commitment with volatile wind power generation," *IEEE Transactions on Power Systems,* vol. 23, pp. 1319-1327, 2008.
[32] S. Shafiee, H. Zareipour, and A. Knight, "Considering thermodynamic characteristics of a CAES facility in self-scheduling in energy and reserve markets," *IEEE Transactions on Smart Grid,* 2016.
[33] Z. Wang and J. Wang, "Self-healing resilient distribution systems based on sectionalization into microgrids," *IEEE Transactions on Power Systems,* vol. 30, pp. 3139-3149, 2015.
[34] Y. Wang, Y. Dvorkin, R. Fernandez-Blanco, B. Xu, T. Qiu, and D. S. Kirschen, "Look-ahead bidding strategy for energy storage," *IEEE Transactions on Sustainable Energy,* vol. 8, pp. 1106-1117, 2017.

[35] H. Sadeghian and M. Ardehali, "A novel approach for optimal economic dispatch scheduling of integrated combined heat and power systems for maximum economic profit and minimum environmental emissions based on Benders decomposition," *Energy,* vol. 102, pp. 10-23, 2016.
[36] M. A. Mirzaei, A. Sadeghi-Yazdankhah, B. Mohammadi-Ivatloo, M. Marzband, M. Shafie-khah, and J. P. Catalão, "Integration of emerging resources in IGDT-based robust scheduling of combined power and natural gas systems considering flexible ramping products," *Energy,* vol. 189, p. 116195, 2019.
[37] M. Khoshjahan, P. Dehghanian, M. Moeini-Aghtaie, and M. Fotuhi-Firuzabad, "Harnessing Ramp Capability of Spinning Reserve Services for Enhanced Power Grid Flexibility," *IEEE Transactions on Industry Applications,* 2019.
[38] http://www.pserc.cornell.edu/matpower/.
[39] H. Khodr, J. Martinez-Crespo, M. Matos, and J. Pereira, "Distribution systems reconfiguration based on OPF using Benders decomposition," *IEEE Transactions on Power Delivery,* vol. 24, pp. 2166-2176, 2009.
[40] B. Moradzadeh and K. Tomsovic, "Mixed integer programming-based reconfiguration of a distribution system with battery storage," in *2012 North American Power Symposium (NAPS)*, 2012, pp. 1-6.
[41] B. Mohammadi-Ivatloo, A. Rabiee, A. Soroudi, and M. Ehsan, "Iteration PSO with time varying acceleration coefficients for solving non-convex economic dispatch problems," *International journal of electrical power & energy systems,* vol. 42, pp. 508-516, 2012.
[42] B. Mohammadi-Ivatloo, M. Moradi-Dalvand, and A. Rabiee, "Combined heat and power economic dispatch problem solution using particle swarm optimization with time varying acceleration coefficients," *Electric Power Systems Research,* vol. 95, pp. 9-18, 2013.
[43] K. T. Chaturvedi, M. Pandit, and L. Srivastava, "Particle swarm optimization with time varying acceleration coefficients for non-convex economic power dispatch," *International Journal of Electrical Power & Energy Systems,* vol. 31, pp. 249-257, 2009.
[44] S. Golshannavaz, S. Afsharnia, and F. Aminifar, "Smart distribution grid: optimal day-ahead scheduling with reconfigurable topology," *IEEE Transactions on Smart Grid,* vol. 5, pp. 2402-2411, 2014.
[45] A. Asrari, T. Wu, and S. Lotfifard, "The impacts of distributed energy sources on distribution network reconfiguration," *IEEE Transactions on Energy Conversion,* vol. 31, pp. 606-613, 2016.
[46] T. T. Nguyen and A. V. Truong, "Distribution network reconfiguration for power loss minimization and voltage profile improvement using cuckoo search algorithm," *International Journal of Electrical Power & Energy Systems,* vol. 68, pp. 233-242, 2015.